



www.sciencemag.org/cgi/content/full/science.1223985/DC1

Supplementary Materials for

A Reversible and Higher-Rate Li-O₂ Battery

Zhangquan Peng, Stefan A. Freunberger, Yuhui Chen, Peter G. Bruce*

*To whom correspondence should be addressed. E-mail: p.g.bruce@st-andrews.ac.uk

Published 19 July 2012 on *Science Express*
DOI: 10.1126/science.1223985

This PDF file includes:

Materials and Methods
Figs. S1 to S9
Full Reference List

Materials and Methods

Materials.

Dimethyl sulfoxide (DMSO) was distilled with addition of NH_2Na then further dried for several days over freshly activated molecular sieves (type 4\AA) resulting in a final water content of ≤ 4 ppm (determined using a Mettler-Toledo Karl Fischer titration apparatus). Battery grade lithium perchlorate (LiClO_4) and lithium bis(trifluoromethane)sulfonimide salt (LiTFSI) were used for preparing the electrolytes as they can be obtained in high purity. Prior to use, both LiClO_4 and LiTFSI were dried by heating under vacuum at $160\text{ }^\circ\text{C}$ for 24 h. 12-Carat white gold leaf (Au:Ag 50:50, m/m), the precursor used to prepare the nanoporous gold (NPG) electrode, was purchased from Noris Blattgold GmbH, Germany. Super P carbon black was obtained from Timcal.

Methods.

Newly polished lithium metal foils (0.38 mm thick from Aldrich) were kept in 0.1 M LiClO_4 -propylene carbonate (PC) electrolyte for at least 3 days before being used as the anode in a Li- O_2 cell containing a 0.1 M LiClO_4 -DMSO electrolyte. This procedure was found to be effective in stabilizing the lithium metal, permitting cycling in DMSO. Before transferring to the cell containing the DMSO electrolyte, the lithium metal was rinsed with DMSO to remove any residual PC.

NPG electrode foils were prepared by dealloying white gold leaf by floating it on a bath of concentrated nitric acid for 5 minutes, following a published procedure (34). This process resulted in a freestanding thin film of NPG. The NPG was dried by heating under vacuum at 150°C overnight. Morphological characterization of NPG by transmission electron microscopy (TEM, Jeol JEM 2011) is shown in Fig. S9. The pore size of NPG is estimated to be 30-50 nm. The cell assembly was conducted in an Ar-

filled glovebox by successively stacking a lithium metal anode, a glass fiber separator (0.3 mm in thickness soaked with ~ 0.1 mL of electrolyte) and a NPG cathode (ranging in mass loading from 0.15 to 5.0 mg/cm²) placed on a stainless steel mesh. To quantify the surface area of the NPG a piece of NPG was mounted on a gold foil (2.0 cm x 2.0 cm x 0.025 mm), and the active surface area was determined by potential scanning between 0.2 and 1.5 V vs. Ag/AgCl in 0.5 M H₂SO₄ according to an established procedure (35). The active area of the NPG cathode was 50 m²/g.

Carbon electrodes composed of Super P:PTFE 8:2, m/m, were prepared by coating pastes composed of carbon, binder, and 2-propanol onto a stainless steel mesh current collector, the mass loading of carbon cathode is typically 1.5 mg/cm². The electrodes were vacuum-dried at 200 °C for 24 hours. Similarly, electrodes containing gold nanoparticles (Super P:PTFE:Au 8:1:1, m/m) were prepared by coating pastes composed of carbon, binder, gold nanoparticles, and 2-propanol onto a stainless steel mesh current collector. The electrodes were first dried at 80 °C for two hours, then vacuum-dried at 200 °C for 24 hours.

FTIR was carried out on a Nicolet 6700 spectrometer (Thermo Fisher Scientific) either in transmission with a CsI pellet or on an ATR unit in a N₂ filled glove box. For the *in situ* SERS the NPG coated gold foil working electrode was placed behind a 1 mm thick sapphire window using a spectroelectrochemical cell described previously (17). Electrochemical measurements were carried out at room temperature using an Autolab PG30 electrochemical workstation. The DEMS system (7, 12) was built in-house and guided by the requirement to quantify all the gases consumed and evolved during the entire discharge and charge cycle. It is based on a commercial quadrupole mass

spectrometer (Thermo Fischer) with turbomolecular pump (Pfeiffer Vacuum) that is backed by a dry scroll pump (Edwards) and leak inlet which samples from the purge gas stream. The cell is based on a customized Swagelok design with polished stainless steel current collectors and double PTFE ferrules to ensure tightness. The cell assembly is as described above. The cathode current collector is integrated with two glued PEEK capillary tubes as purge gas inlet and outlet. The headspace above the cathode is ca 400 μL . The purge gas system consists of a gas cylinder, a digital mass flow controller (Bronkhorst), PEEK or stainless steel capillary tubing, a high pressure 2-position 6-port GC valve that allows for transfer from the glovebox without air exposure (all Valco), a T-piece where the MS samples and an outlet check valve (Swagelok) with an additional capillary to avoid back diffusion. Tightness was checked by Helium leak testing by means of the MS. Purge gas flows were typically 0.3 mL/min. The setup was calibrated for Ar, O₂, CO₂, H₂, N₂ and H₂O using calibration mixtures in steps over the anticipated concentration ranges to capture nonlinearity and cross-sensitivity (0-10% Ar/O₂ in each other plus 0-10000ppm of the other gases). Detection limits are <1 ppm. For typical discharge/charge currents relative gas evolution corresponding to < 0.1 % of the O₂ consumed/evolved is readily detected. Ultrapure He was used for the background. All calibration and quantification was performed using in-house software. Two working modes of the DEMS setup are used: a) Ar as carrier gas is used for detection of all gases evolved on charging, and b) In order to quantify O₂ consumption on discharge whilst measuring any gases evolved a mixture of ca. 5 % Ar in O₂ is used as the carrier gas. Ar acts as tracer gas with known invariable flux. As in a) the measured concentrations allow calculation of the flux of each component.

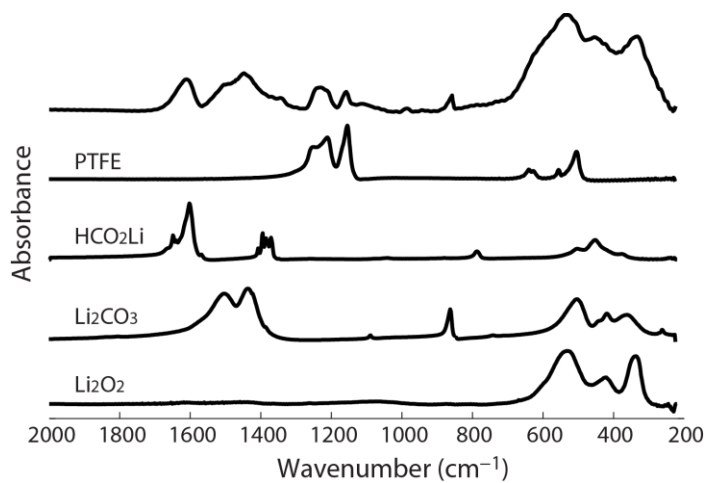


Fig. S1

FTIR data from a Super P carbon based cathode at the end of 1st discharge in 0.1 M LiPF₆-DME (dimethoxyethane) showing significant electrolyte decomposition. Such decomposition is not evident in powder X-ray diffraction due to poor crystallinity of the decomposition products, it is necessary to use techniques such as FTIR/NMR to observe the problems of ether electrolytes.

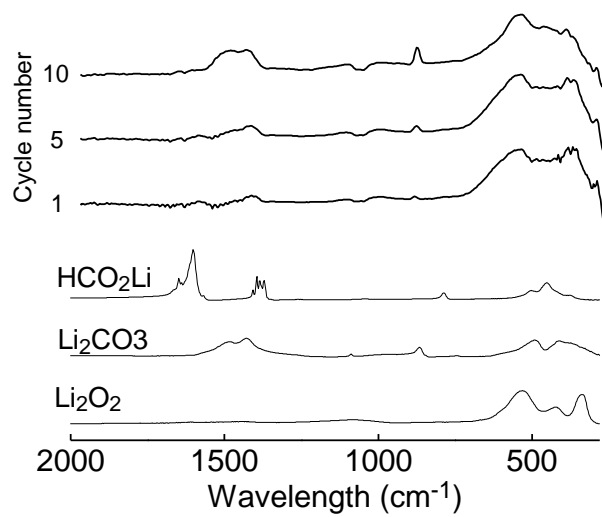


Fig. S2

FTIR spectra of a discharged NPG cathode in 0.1 LiPF₆-DME as function of cycle number, showing increasing growth of side-reaction products with cycling.

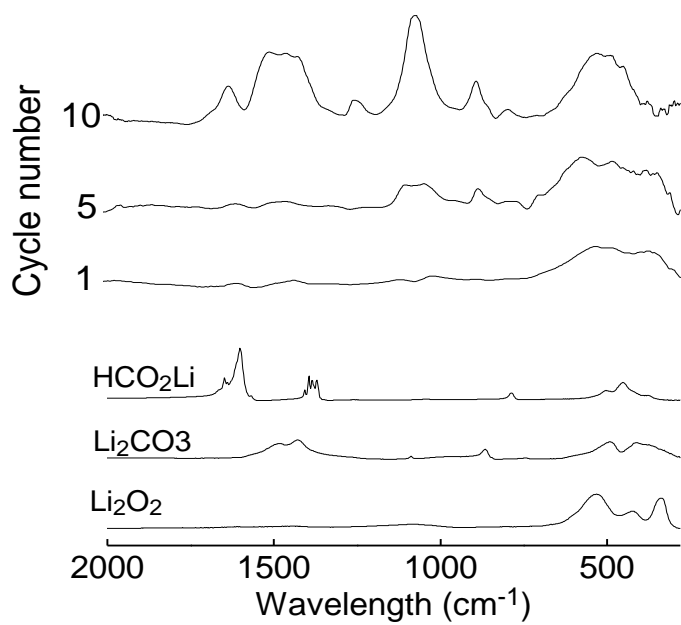


Fig. S3

FTIR spectra of a discharged NPG cathode in 0.1 LiPF₆-tetraglyme as function of cycle number. Bands are consistent with those observed for tetraglyme in ref 12.

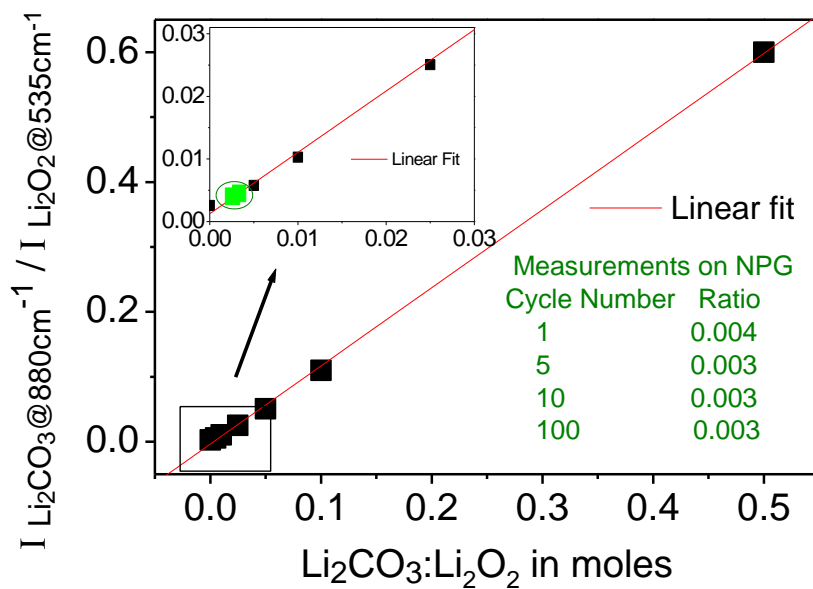


Fig. S4

FTIR calibration curve obtained by mixing known amounts of Li_2CO_3 and Li_2O_2 with different ratios. Note that the isolated Li_2CO_3 peak at 880 cm^{-1} was chosen in order to avoid interference from lithium formate. Inset shows expansion of the low ratio range. The green circle highlights the values obtained from the discharged NPG electrodes on different cycles.

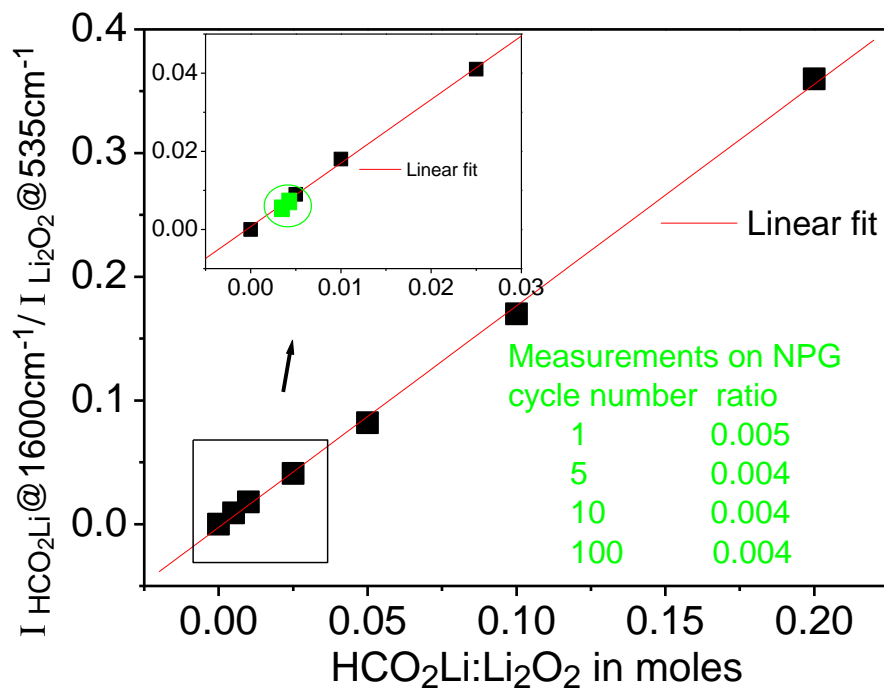


Fig. S5

FTIR calibration curve obtained by mixing known amounts of HCO₂Li and Li₂O₂ with different ratios. Note that the isolated HCO₂Li peak at 1600 cm⁻¹ was chosen in order to avoid interference from lithium carbonate. Inset shows expansion of the low ratio range. The green circle highlights the values obtained from the discharged NPG electrodes on different cycles.

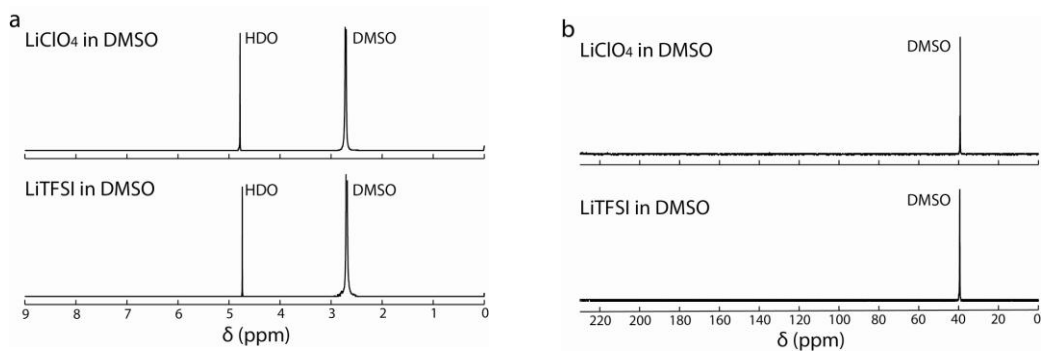


Fig. S6

(a) ¹H and (b) ¹³C NMR data of 0.1 M LiClO₄-DMSO and LiTFSI-DMSO electrolytes used for a Li-O₂ cell with NPG cathode, after 100 discharge and charge cycles.

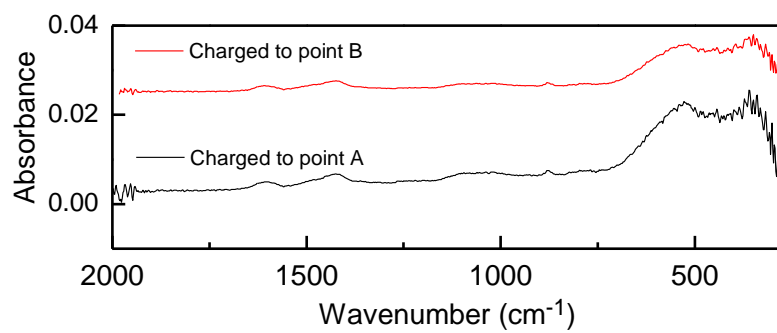


Fig. S7

FTIR spectra from a NPG electrode at the states of charge indicated by A and B in Fig. 1.

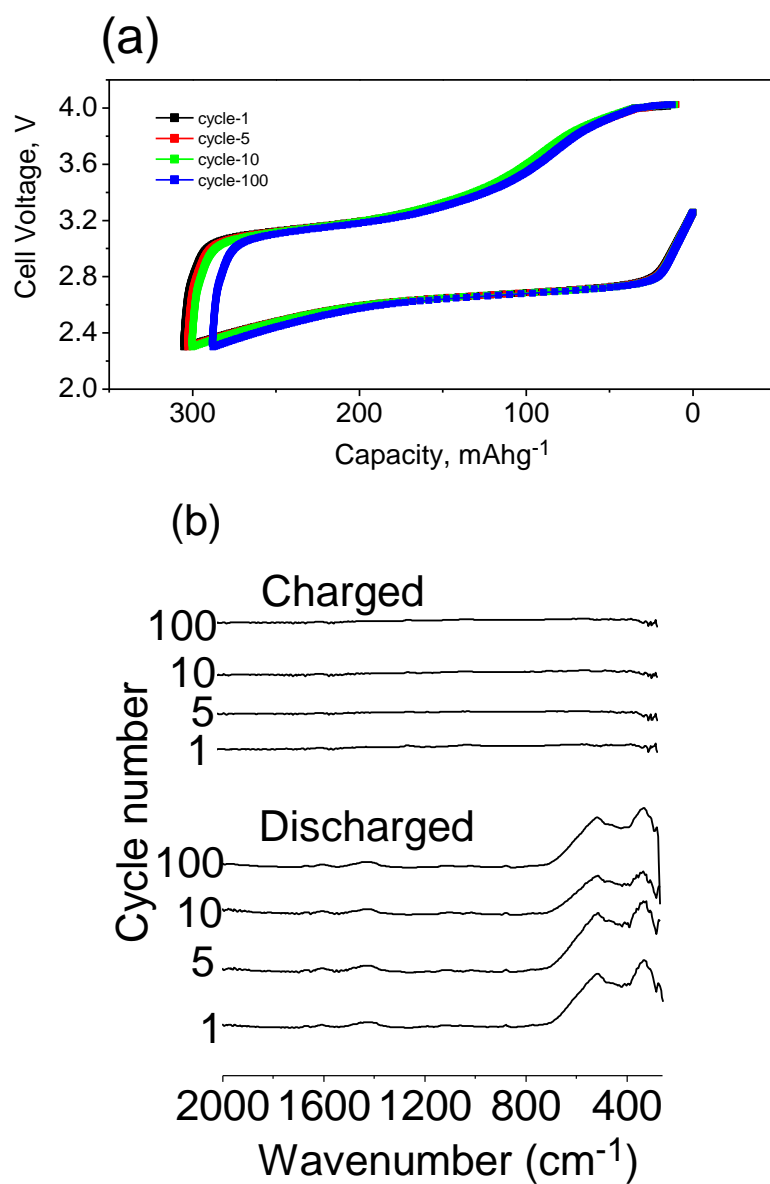


Fig. S8

(a) Discharge-charge curves of NPG cathode in oxygen saturated 0.1 M LiTFSI-DMSO electrolyte at a current density of 500 mA g⁻¹. (b) FTIR of NPG cathode as function of cycle number.

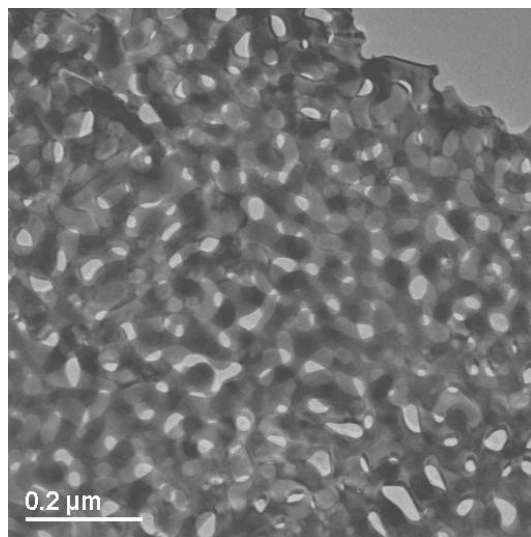


Fig. S9
TEM image of NPG.

References and Notes

1. K. M. Abraham, Z. Jiang, A polymer electrolyte-based rechargeable lithium/oxygen battery. *J. Electrochem. Soc.* **143**, 1 (1996). [doi:10.1149/1.1836378](https://doi.org/10.1149/1.1836378)
2. P. G. Bruce, S. A. Freunberger, L. J. Hardwick, J.-M. Tarascon, Li-O₂ and Li-S batteries with high energy storage. *Nat. Mater.* **11**, 19 (2012). [doi:10.1038/nmat3191](https://doi.org/10.1038/nmat3191) [Medline](#)
3. G. Girishkumar, B. McCloskey, A. C. Luntz, S. Swanson, W. Wilcke, Lithium-air battery: Promise and challenges. *J. Phys. Chem. Lett.* **1**, 2193 (2010). [doi:10.1021/jz1005384](https://doi.org/10.1021/jz1005384)
4. B. Scrosati, J. Hassoun, Y.-K. Sun, Lithium-ion batteries. A look into the future. *Energy Environ. Sci.* **4**, 3287 (2011). [doi:10.1039/c1ee01388b](https://doi.org/10.1039/c1ee01388b)
5. J.-G. Zhang, P. G. Bruce, X. G. Zhang, "Metal-air batteries," in *Handbook of Battery Materials*, C. Daniel, J. O. Besenhard, Eds. (Wiley-VCH Verlag GmbH & Co. KGaA, Weinheim, Germany, ed. 2, 2011).
6. J. Christensen *et al.*, A critical review of Li/air batteries. *J. Electrochem. Soc.* **159**, R1 (2012). [doi:10.1149/2.086202jes](https://doi.org/10.1149/2.086202jes)
7. S. A. Freunberger *et al.*, Reactions in the rechargeable lithium-O₂ battery with alkyl carbonate electrolytes. *J. Am. Chem. Soc.* **133**, 8040 (2011). [doi:10.1021/ja2021747](https://doi.org/10.1021/ja2021747) [Medline](#)
8. F. Mizuno, S. Nakanishi, Y. Kotani, S. Yokoishi, H. Iba, Rechargeable Li-air batteries with carbonate-based liquid electrolytes. *Electrochemistry* **78**, 403 (2010). [doi:10.5796/electrochemistry.78.403](https://doi.org/10.5796/electrochemistry.78.403)
9. W. Xu *et al.*, Investigation on the charging process of Li₂O₂-based air electrodes in Li-O₂ batteries with organic carbonate electrolytes. *J. Power Sources* **196**, 3894 (2011). [doi:10.1016/j.jpowsour.2010.12.065](https://doi.org/10.1016/j.jpowsour.2010.12.065)
10. G. M. Veith, N. J. Dudney, J. Howe, J. Nanda, Spectroscopic characterization of solid discharge products in Li-air cells with aprotic carbonate electrolytes. *J. Phys. Chem. C* **115**, 14325 (2011). [doi:10.1021/jp2043015](https://doi.org/10.1021/jp2043015)
11. B. D. McCloskey, D. S. Bethune, R. M. Shelby, G. Girishkumar, A. C. Luntz, Solvents' critical role in nonaqueous lithium-oxygen battery electrochemistry. *J. Phys. Chem. Lett.* **2**, 1161 (2011). [doi:10.1021/jz200352v](https://doi.org/10.1021/jz200352v)
12. S. A. Freunberger *et al.*, The lithium-oxygen battery with ether-based electrolytes. *Angew. Chem. Int. Ed.* **50**, 8609 (2011). [doi:10.1002/anie.201102357](https://doi.org/10.1002/anie.201102357) [Medline](#)
13. H. Wang, K. Xie, Investigation of oxygen reduction chemistry in ether and carbonate based electrolytes for Li-O₂ batteries. *Electrochim. Acta* **64**, 29 (2012). [doi:10.1016/j.electacta.2011.12.080](https://doi.org/10.1016/j.electacta.2011.12.080)
14. H.-G. Jung, J. Hassoun, J.-B. Park, Y.-K. Sun, B. Scrosati, An improved high-performance lithium-air battery. *Nat. Chem.* **4**, 579 (2012). [doi:10.1038/nchem.1376](https://doi.org/10.1038/nchem.1376) [Medline](#)
15. Materials and methods are available as supplementary materials on *Science Online*.
16. C. O. Laoire, S. Mukerjee, K. M. Abraham, E. J. Plichta, M. A. Hendrickson, Influence of nonaqueous solvents on the electrochemistry of oxygen in the rechargeable lithium-air battery. *J. Phys. Chem. C* **114**, 9178 (2010). [doi:10.1021/jp102019y](https://doi.org/10.1021/jp102019y)

17. Z. Peng *et al.*, Oxygen reactions in a non-aqueous Li⁺ electrolyte. *Angew. Chem. Int. Ed.* **50**, 6351 (2011). [doi:10.1002/anie.201100879](https://doi.org/10.1002/anie.201100879) [Medline](#)
18. B. D. McCloskey *et al.*, Twin problems of interfacial carbonate formation in nonaqueous Li–O₂ batteries. *J. Phys. Chem. Lett.* **3**, 997 (2012). [doi:10.1021/jz300243r](https://doi.org/10.1021/jz300243r)
19. A. Débart, A. J. Paterson, J. Bao, P. G. Bruce, α -MnO₂ nanowires: A catalyst for the O₂ electrode in rechargeable lithium batteries. *Angew. Chem. Int. Ed.* **47**, 4521 (2008). [doi:10.1002/anie.200705648](https://doi.org/10.1002/anie.200705648) [Medline](#)
20. C. J. Allen, S. Mukerjee, E. J. Plichta, M. A. Hendrickson, K. M. Abraham, Oxygen electrode rechargeability in an ionic liquid for the Li–air battery. *J. Phys. Chem. Lett.* **2**, 2420 (2011). [doi:10.1021/jz201070t](https://doi.org/10.1021/jz201070t)
21. Y.-C. Lu *et al.*, The discharge rate capability of rechargeable Li–O₂ batteries. *Energy Environ. Sci.* **4**, 2999 (2011). [doi:10.1039/c1ee01500a](https://doi.org/10.1039/c1ee01500a)
22. Y.-C. Lu, H. A. Gasteiger, Y. Shao-Horn, Catalytic activity trends of oxygen reduction reaction for nonaqueous Li–air batteries. *J. Am. Chem. Soc.* **133**, 19048 (2011). [doi:10.1021/ja208608s](https://doi.org/10.1021/ja208608s) [Medline](#)
23. T. Ogasawara, A. Débart, M. Holzapfel, P. Novák, P. G. Bruce, Rechargeable Li₂O₂ electrode for lithium batteries. *J. Am. Chem. Soc.* **128**, 1390 (2006). [doi:10.1021/ja056811q](https://doi.org/10.1021/ja056811q) [Medline](#)
24. B. D. McCloskey *et al.*, On the efficacy of electrocatalysis in nonaqueous Li–O₂ batteries. *J. Am. Chem. Soc.* **133**, 18038 (2011). [doi:10.1021/ja207229n](https://doi.org/10.1021/ja207229n) [Medline](#)
25. S. J. Visco, B. D. Katz, Y. S. Nimon, L. D. DeJonghe, U.S. Patent 7,282,295, 2007.
26. X.-H. Yang, P. He, Y.-Y. Xia, Preparation of mesocellular carbon foam and its application for lithium/oxygen battery. *Electrochem. Commun.* **11**, 1127 (2009). [doi:10.1016/j.elecom.2009.03.029](https://doi.org/10.1016/j.elecom.2009.03.029)
27. J. Read, Characterization of the lithium/oxygen organic electrolyte battery. *J. Electrochem. Soc.* **149**, A1190 (2002). [doi:10.1149/1.1498256](https://doi.org/10.1149/1.1498256)
28. Y. G. Wang, H. S. Zhou, A lithium–air battery with a potential to continuously reduce O₂ from air for delivering energy. *J. Power Sources* **195**, 358 (2010). [doi:10.1016/j.jpowsour.2009.06.109](https://doi.org/10.1016/j.jpowsour.2009.06.109)
29. J. S. Hummelshøj *et al.*, Elementary oxygen electrode reactions in the aprotic Li–air battery. *J. Chem. Phys.* **132**, 071101 (2010). [doi:10.1063/1.3298994](https://doi.org/10.1063/1.3298994) [Medline](#)
30. V. S. Bryantsev, M. Blanco, F. Faglioni, Stability of lithium superoxide LiO₂ in the gas phase: computational study of dimerization and disproportionation reactions. *J. Phys. Chem. A* **114**, 8165 (2010). [doi:10.1021/jp1047584](https://doi.org/10.1021/jp1047584) [Medline](#)
31. Y. Mo, S. P. Ong, G. Ceder, First-principles study of the oxygen evolution reaction of lithium peroxide in the lithium–air battery. *Phys. Rev. B* **84**, 205446 (2011). [doi:10.1103/PhysRevB.84.205446](https://doi.org/10.1103/PhysRevB.84.205446)
32. D. Aurbach, M. Daroux, P. Faguy, E. Yeager, The electrochemistry of noble metal electrodes in aprotic organic solvents containing lithium salts. *J. Electroanal. Chem.* **297**, 225 (1991). [doi:10.1016/0022-0728\(91\)85370-5](https://doi.org/10.1016/0022-0728(91)85370-5)

33. J. Hassoun, F. Croce, M. Armand, B. Scrosati, Investigation of the O₂ electrochemistry in a polymer electrolyte solid-state cell. *Angew. Chem. Int. Ed.* **50**, 2999 (2011).
[doi:10.1002/anie.201006264](https://doi.org/10.1002/anie.201006264) [Medline](#)
34. Y. Ding, Y.-J. Kim, J. Erlebacher, Nanoporous gold leaf: “Ancient technology”/advanced material. *Adv. Mater.* **16**, 1897 (2004). [doi:10.1002/adma.200400792](https://doi.org/10.1002/adma.200400792)
35. R. Woods, in *Electroanalytical Chemistry, A Series of Advances*, A. J. Bard, Ed., vol. 9 (Marcel Dekker, New York, 1976).